Reports

High-Temperature Cubic Boron Nitride P-N Junction Diode Made at High Pressure

OSAMU MISHIMA, JUNZO TANAKA, SHINOBU YAMAOKA,
OSAMU FUKUNAGA*

A p-n junction diode of cubic boron nitride was made by growing an n-type crystal epitaxially on a p-type seed crystal at a pressure of 55 kilobars and a temperature of about 1700°C. A temperature-difference solvent method was used for the crystal growth, and beryllium and silicon were doped as acceptors and donors, respectively. Formation of the p-n junction was clearly confirmed at 1 bar by rectification characteristics and by existence of a space charge layer of the junction as observed by electron beam induced current measurement. This diode operated at 530°C.

MATERIALS MADE OF TETRAHEDRALLY bonded light elements, such as diamond and cubic boron nitride, may be useful as large energy-gap semiconductors. Cubic boron nitride (cBN), the simplest III-V compound and one that is stable under high pressure and metastable to about 1300°C at 1 bar (*1*), has the widest energy gap [>6.4 eV (*2*)] among IV and III-V materials. Electronic devices made of cBN are therefore likely to operate at high temperatures. Different from diamond, which cannot easily be made into an n-type semiconductor (*3*, *4*), cBN can be made into both p- and n-type semiconductors when suitable impurities are added (*5*). Although there was an attempt to produce bulk p-n junctions of cBN under pressure, the prepared composite samples were too small to be studied because of difficulties with the growth of cBN crystals (*5*). We have now successfully fabricated large cBN crystals in our laboratory by a temperature-difference solvent method (*6*). In this report, relatively large cBN p-n junction diodes were made under pressure by means of this growth method and examined at 1 bar.

The temperature-difference solvent method may be described as follows: cBN powder is placed at the high-temperature end of a growth cell, which is made of molybdenum, and the cell is placed in a high-pressure oven. The powder melts into a $LiCaBN_2$ solvent, and large single crystals of cBN precipitate at the low-temperature end of the cell (*6*).

When about 1% by weight of beryllium metal—a p-type dopant for cBN (*5*)—was added to the solvent, dark blue, polyhedral, and electrically conductive (10^2 to 10^3 ohms) cBN crystals (about 1 mm in size) precipitated after about 20 hours under 55 kbar and at ~1700°C. As Wentorf observed (*5*), the larger the amount of beryllium in the cell, the darker the blue color of cBN; the color sometimes did not distribute uniformly in the crystal.

In a subsequent run with another growth cell, a few dark blue p-type cBN crystals with dimensions of about 0.5 to 1.0 mm were placed at the low-temperature end of the cell as seed crystals. When about 5% by weight of silicon—an n-type dopant (*5*)—was added to the solvent, yellow orange, polyhedral and electrically conductive (10^3 to 10^4 ohms) cBN crystals with maximum thickness of about 0.5 mm were grown on the blue seed after about 20 hours under 55 kbar and 1700°C. Some n-type crystals were also made by spontaneous nucleation. The p-n composite crystals of about 1 mm in total size had the appearance of a tiny boiled egg that consists of a dark blue p-type region in the center and a yellow-orange n-type region around it. An interface between the p- and the n-type regions, which could be seen through the transparent n-type crystal, was round because of slight melting of the seed crystal in an initial stage of crystal growth; there were a few small pools of trapped solvents near the p-n interface. A lack of uniformity of the yellow-orange color in some n-type crystals, which formed dark brown areas, was also observed.

Two of these p-n composite samples were formed into slabs by grinding the crystals with a diamond wheel of 800 mesh to expose the inner p-type region, which provided electrical contact for measurements, and the undesirable solvent pools near the interface were eliminated. One sample fractured almost vertically with respect to the p-n interface during the grinding. The cleavage surface was smooth and flat over the p-n boundary, as observed by a scanning electron microscope: the whole sample was a single crystal, although epitaxial growth on a seed was confirmed by x-ray analysis on a similar sample.

Since methods for making ohmic contacts to cBN have not yet been developed, electrical measurement on one of the p-n composite crystals and on the p- and n-type crystals was made by means of a four-point probe method to eliminate problems of metal-semiconductor contact barriers. Silver-painted electrodes were used and distances between the terminals were 0.2 to 0.5 mm. The electric power supplied to the samples was carefully limited, usually to less than 0.1 mW, depending on conditions of the electrodes, to avoid the increase of sample temperature that mainly arises from both large contact resistance (about 1 megohm at room temperature) at the current electrodes and small size (about 0.1 mg) of the samples. A direct current was used to minimize effect of capacitance at the voltage terminals.

Typical results of the electric measurement up to about 600°C are shown in Figs. 1 and 2. The p-n composite sample showed the usual rectification characteristics (Fig. 1). Although *V-I* (voltage-current) characteristics differed slightly depending on the location and polarity of the electrodes, the same rectification characteristics were always observed when the current passed through the junction. A small amount of leakage current flowed in the reverse direction and

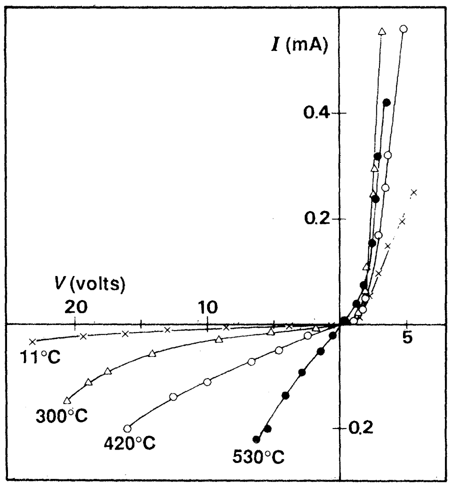

Fig. 1. Typical rectification characteristics and temperature dependence of the cBN p-n junction diode. The actual sample temperature might be slightly higher because of the large supplied power.

National Institute for Research in Inorganic Materials, 1-1 Namiki, Sakura-mura, Niihari-gun, Ibaraki 305, Japan.

*Present address: Department of Engineering, Tokyo Institute of Technology, 2-12 Ookayama, Meguroku, Tokyo 152, Japan.

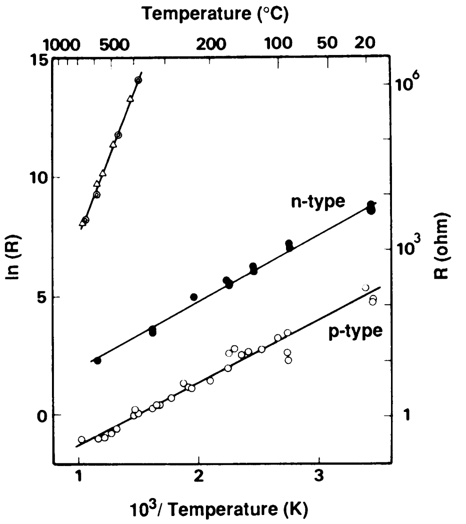

Fig. 2. Temperature dependence of resistance of cBN crystals: (○) the Be-doped p-type crystal; (●) the Si-doped n-type crystal; (△) the high-resistance region of the n-type crystal; (⊙) the undoped yellow crystal.

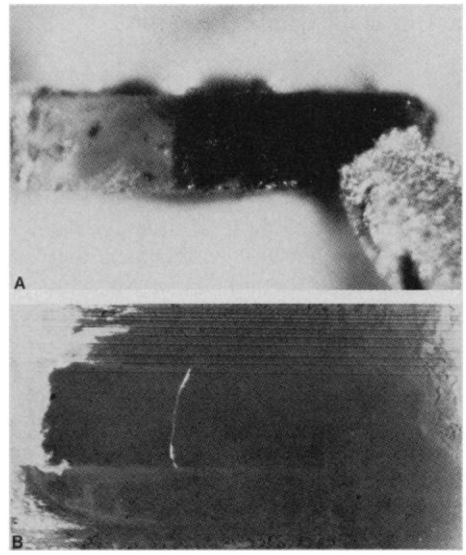

Fig. 3. The cBN p-n junction diode. (**A**) A photograph of the cleavage surface of the diode with two electrodes for EBIC measurement. The dark right-hand side of the sample corresponds to the p-type region and the left-hand side to the n-type region. (**B**) An EBIC picture of the same diode. If an electron beam is injected into a crystal, a large number of excited electrons and holes are produced only inside the electric field of a space-charge layer in the crystal and these carriers can induce a short-circuit current. By scanning the micro-focused electron beam on the sample and detecting intensity and direction of the induced current, the location of the space charge layer, as well as its electrical polarity, can be measured. The space-charge region is the bright line in this picture.

the amount increased monotonically with increased temperature as shown in the same figure. These reproducible rectification characteristics were observed at 530°C.

Good linear *V-I* characteristics were observed for the p- and n-type crystals, owing to the four-point probe method, and the effects of temperature on their resistance are shown in Fig. 2. Activation energy of the measured p-type crystal, estimated from the slope in the figure, was 0.23 ± ~0.02 eV and that of the n-type crystal was 0.24 ± ~0.03 eV. The activation energy of the n-type crystal was reconfirmed by using pure n-type crystals grown without any beryllium impurity in the growth cell. Electrical conductivity was difficult to measure because of a lack of uniformity of the resistance in the crystals, and the mobility and amount of doping were not estimated.

Besides the above p- and n-type activation centers, another deeper activation center was found by the measurement on high-resistance regions of the n-type crystals and on undoped yellow crystals, as shown in Fig. 2. The activation energy was estimated to be 1.11 ± ~0.15 eV from the slope in the figure. The *V-I* measurement on the n-type crystals and on the p-n composite crystal became difficult above about 600°C because of instability of the sample resistance.

It was also clearly shown from electron beam–induced current (EBIC) measurement (*7, 8*) that the rectification characteristics originated from the p-n junction. Figure 3A shows the cleavage surface that had the p-n interface aligned almost vertically, and Fig. 3B shows the EBIC picture taken of the surface at room temperature. The bright continuous line across the sample indicates the existence of a space-charge layer in the crystal. This space-charge layer agreed exactly with the p-n space-charge layer that we expected would exist along the boundary between the blue p-type and the yellow orange n-type regions if the junction was really formed. The EBIC flowed from the n-type to the p-type region by way of the junction and there was no other detectable space-charge layer in the crystal. These results confirmed formation of the p-n junction of cBN. Width of the junction was less than about 2000 Å, which was the maximum resolution in the present EBIC measurement system. The same continuous EBIC line was also observed on the ground surface of the other sample that was used for the resistance measurement.

Application of high pressure has in the past usually been restricted to producing diamond and cBN as superhard and thermally conductive materials, although simple thermistors of diamond and cBN have been patented (*9*). Our p-n junction diode could be made by the temperature-difference solvent method under high pressure, and to our knowledge it is the first example of the fabrication of a complicated electronic device under such extreme conditions.

The p-n junction diode was made of the simplest III-V compound with the largest energy gap and it was functional at 530°C. In principle, an ideal cBN diode should operate up to about 1300°C, the temperature at which cBN becomes thermally unstable. The observed leakage currents in the reverse direction were responsible for the low operation temperature of 530°C, although the temperature and estimated reverse current density (about 0.1 A/cm^2 at a reverse bias of 3 V at 530°C) were comparable to those of the highest temperature semiconductor devices existing at present (*10, 11*). These leakage currents might be related to a deep level. Although the origin of the deep level is unknown, the rectification characteristics at high temperatures might be improved with more refined samples. Purification and perfection of the samples was not optimum in the present experiment; the generation of carriers, caused by defects and uncertain impurities, might be occurring in the present samples. There is still a possibility that the cBN devices made under pressure can be used as much higher temperature electronic components.

In addition to the large energy gap, cBN is thought to have other extraordinary properties, such as high thermal conductivity [about 13 W cm^{-1} deg^{-1} at 25°C (*12*)] and low dielectric constants [$\varepsilon_0 = 7.1$, $\varepsilon_\infty = 4.5$ (*13*) the zero-frequency and infinite-frequency constants, respectively], which are advantageous for electronic devices. When ohmic contact and other related technical improvements are achieved, broad application of the cBN semiconductor will be possible, allowing the fabrication of special high-temperature and wide-gap semiconductor devices.

REFERENCES AND NOTES

1. R. C. DeVries, *Report No. 72 CRD 178* (General Electric Corporation, Schenectady, NY, 1972).
2. R. M. Chrenko, *Solid State Commun.* **14**, 511 (1974).

3. R. H. Wentorf, Jr., *J. Chem. Phys.* **36**, 1987 (1962).
4. A. T. Collins and E. C. Lightowlers, in *The Properties of Diamond*, J. E. Field, Ed. (Academic Press, London, 1979), pp. 79–105.
5. R. H. Wentorf, Jr., *J. Chem. Phys.* **36**, 1990 (1962).
6. O. Mishima, S. Yamaoka, O. Fukunaga, *J. Appl. Phys.* **61**, 2822 (1987).
7. F. Berz and H. K. Kuiken, *Solid-State Electron.* **19**, 437 (1976).
8. C. A. Dimitriadis, *IEEE Trans. Electron Devices* **ED-32**, 1761 (1985).
9. H. P. Bovenkerk, U.S. Patent 3735321 (1973).
10. T. E. Zipperian, L. R. Dawson, C. E. Barnes, *Appl. Phys. Lett.* **40**, 901 (1982).
11. T. E. Zipperian and L. R. Dawson, *J. Appl. Phys.* **54**, 6019 (1983).
12. G. A. Slack, *J. Phys. Chem. Solids* **34**, 321 (1973).
13. P. J. Gielisse *et al.*, *Phys. Rev.* **155**, 1039 (1967).

14. We thank M. Tsutsumi for the EBIC measurement.

8 June 1987; accepted 5 August 1987

Organic Matter on Asteroid 130 Elektra

D. P. Cruikshank and R. H. Brown

Infrared absorption spectra of a low-albedo water-rich asteroid appear to show a weak 3.4-micrometer carbon-hydrogen stretching mode band, which suggests the presence of hydrocarbons on asteroid 130 Elektra. The organic extract from the primitive carbonaceous chondritic Murchison meteorite shows similar spectral bands.

THE CARBONACEOUS CHONDRITIC meteorites are known to contain organic matter. Aliphatic and aromatic polymers constitute about 6% of the mass of the volatile-rich CI chondrites, which are among the most primitive samples of matter in the solar system. These meteorites represent a low-temperature condensate from the solar nebula and contain all of the stable elements in solar proportions except for the highly volatile major elements hydrogen, carbon, nitrogen, and oxygen, and the noble gases (*1–3*). The parent body or bodies of the CI carbonaceous chondrites have been affected by liquid water, as evidenced by the clays and other aqueous alteration products found in the meteorites.

Several investigations have shown the apparent connections between various kinds of meteorites and certain classes of asteroids (*4–6*) in the main belt, and more recently the connection has been drawn even closer by finding meteorite analogs among the planet-crossing asteroids (*7, 8*). This latter step is important in understanding the details of transport of material from apparently stable asteroid orbits to Earth (*9, 10*).

Although the carbonaceous chondrite parent bodies are presumed to exist among the outer asteroids, the evidence is based on their mutual low albedos and, in some cases, reddish color. Lebofsky *et al.* (*11*) have shown that some, but not all, low-albedo C-type asteroids have a broad absorption in their spectra at 3 μm that is attributable to bound water in the mineral lattices. This finding is consistent with the bound water in the CI and CM carbonaceous chondrites. The strength of the ultraviolet absorption, attributed to charge-transfer transitions in iron and titanium, is related to the amount of water represented by the 3-μm absorption (*12*).

In the primitive carbonaceous chondrites, such as Orgueil (CI), Murray (CM), and Murchison (CM), a complex of very shallow bands at 3.4 μm is superimposed on the 3-μm bound-water band seen in diffuse reflectance. These features are caused by the C–H stretching mode and are common to all organic matter, although the exact positions and band shapes vary among compounds. Other classes of carbonaceous chondrites, such as Allende (CV), do not show the C–H band clearly, nor do they have significant bound water evident in their reflectance spectra.

We have sought to carry the connection between the most primitive carbonaceous chondrites and the asteroids further by searching for the C–H organic band in asteroid spectra. In August 1986, we used the cooled-grating array spectrometer (CGAS) at the NASA Infrared Telescope Facility at Mauna Kea, Hawaii, to obtain spectra of asteroid 130 Elektra. Figure 1 shows the asteroid spectrum in the region of the 3.4-μm band. In Fig. 1, curve b, the spectrum is shown as the simple ratio to the spectrum of a solar-type star (Fig. 1, curve e) (*13*). For comparison, the laboratory reflectance spectrum of the insoluble organic extract from the Murchison Cl carbonaceous chondrite is shown (Fig. 1, curve a). The complex of bands at 3.4 μm in the meteorite sample is due to the C–H stretching mode in the organic compounds in the extract. The spectrum of the bulk Murchison meteorite also shows the C–H band, as well as the 3-μm bound-water absorption. Depending on the particle size and packing of the laboratory samples, the band strengths in the bulk meteorite can appear as strong as those in the concentrated organic residue (*14*). Figure 1, curves c and d, shows the same two spectra, but with the continua removed computationally by means of a cubic spline fit to points on the spectrum that were assumed to represent the local

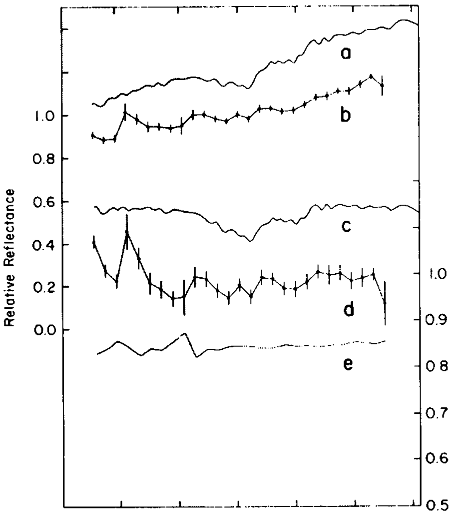

Fig. 1. Reflectance spectra of asteroid 130 Elektra and an organic extract from the Murchison carbonaceous chondrite meteorite. Curve a is the spectrum of Murchison with two times vertical exaggeration to emphasize the weak features between 3.35 and 3.55 μm. Curve b is the telescopic spectrum of 130 Elektra (no exaggeration) with error bars (1σ) as shown. This spectrum is the ratio of the asteroid to the spectrum of the standard star. Curve c is the Murchison spectrum with the continuum slope removed computationally, and curve d is the Elektra spectrum similarly flattened (and with two times vertical exaggeration). Curve e is the standard star spectrum (corrected for extinction). At wavelengths shorter than 3.35 μm, atmospheric extinction is very strong and cannot be entirely removed, as shown in the star spectrum (curve e). The portions of the spectra in the hatched area are, therefore unreliable. At wavelengths longer than 3.35 μm, as seen in the very clean stellar spectrum, correction for atmospheric extinction is very good, and spectral features in the asteroid data can be judged on the basis of their correspondence with similar features in the laboratory spectrum of the meteorite sample. The ordinate scale on the left pertains to spectrum b, whereas that on the right pertains to spectrum d. The other spectra have been offset vertically for clarity.

D. P. Cruikshank, Institute for Astronomy. Honolulu, HI 96822.
R. H. Brown, Jet Propulsion Laboratory, Pasadena, CA 91109.